



2  
3  
4  
5  
6  
7 **Supplementary Information for**

8 Specification of neuronal subtypes in the spiral ganglion begins prior  
9 to birth in the mouse

10  
11 Tessa R. Sanders<sup>1\*</sup> and Matthew W. Kelley<sup>1\*</sup>

12  
13 \*Corresponding authors: Tessa R. Sanders and Matthew W. Kelley

14 Email: [tessa.sanders@nih.gov](mailto:tessa.sanders@nih.gov) and [kelleymt@nidcd.nih.gov](mailto:kelleymt@nidcd.nih.gov)

15  
16  
17 **This PDF file includes:**

18  
19       Supplementary methods

20       Figures S1 to S12

21       Tables S1 to S2

22  
23 **Other supplementary materials for this manuscript include the following:**

24  
25       Datasets S1 to S8

30 **Supplementary methods**

31 Animals: All mice were maintained within the Porter Neuroscience Research Center Shared Animal  
32 Facility. All animal care and housing was conducted in accordance with the NIH guidelines for  
33 animal use (Protocols 1254 and 1262). Randomly selected mice of either sex were used in all  
34 experiments. Timed-pregnant CD1 females were obtained from Charles River. Ngn1<sup>creErt2</sup> mice  
35 were obtained from Dr. Lisa Goodrich, Harvard Medical School(1) and Tac1Cre and MAPT<sup>EGFP</sup>  
36 mice were obtained from The Jackson Laboratory (Strain #021877(2) and strain # 004779 (3)), and  
37 were maintained on a mixed background.

38

39 Tissue collection: At E14, E16, and E18, pregnant CD1 females were euthanized and cochleae  
40 were dissected from 5 embryos. At P1, 5 pups were euthanized and cochleae were collected. At  
41 all ages spiral ganglia (SG) were grossly dissected out of the cochlea with some sensory epithelia  
42 and mesenchyme still attached. At E16 SG were separated into basal and apical portions by cutting  
43 through the middle turn. At E14, E16 and E18, three biological replicates were collected containing  
44 pooled tissue from separate litters. At P1, two biological replicates were collected.

45 Dissociation of SGNs at E14 and E16 : Pooled SG were dissociated for 14 minutes in 0.05%  
46 Trypsin-EDTA at 37°C, with two vigorous triturations. Trypsin was neutralized with the addition of  
47 an equal volume of FBS.

48 Dissociation of SGNs at E18 and P1: Pooled SG were dissociated for 25 minutes in Papain  
49 (20U/mL) at 37°C, with triturations every 5 mins. Papain was neutralized with the addition of  
50 Ovomuroid inhibitor.

51 Regardless of age of dissection, dissociated cells were passed through a 20µm strainer, spun down  
52 at 300 x g and then resuspended in PBS with 0.4mg/mL BSA and 0.2U/mL RNase inhibitor at a  
53 density of 1,100 cells/ml. Single cells from the dissociated preparations were captured on the 10X  
54 Genomics Chromium Controller, followed by lysis, conversion of mRNA to cDNA, and preparation  
55 of sequencing libraries using Chromium Single Cell 3' Reagents (v3.1) and the manufacturer's

56 suggested protocols. Libraries were sequenced on an Illumina NextSeq and were aligned to the  
57 Ensembl mouse MM10 assembly using Cell Ranger 3.0.1 analysis software (10X Genomics).  
58  
59 Initial data processing: Initial 'mean reads per cell', 'median genes per cell' and 'number of reads'  
60 data from the Cell Ranger output is available in Suppl data file 8. Further processing of individual  
61 datasets was carried out in Seurat (R package, v3.2)(4). Briefly, Cell Ranger outputs were imported  
62 into Seurat using the 'Read10x' function. Genes present in fewer than 3 cells, cells with fewer than  
63 200 unique genes identified, and cells with more than 15,000 total RNA molecules detected were  
64 all removed from the analysis. Cells with higher than 5% mitochondrial or hemoglobin transcripts  
65 (*Hba-a1*, *Hba-a2*, *Hbb-bh1*, *Hbb-bs*, *Hbb-bt*) were also removed to avoid contamination with  
66 dead/dying cells, or red blood cells. Data were normalized, scaled and dimensionally reduced using  
67 the standard Seurat workflow. In order to detect doublets within the dataset we used DoubletFinder  
68 (R package, v2.0.3) (5) with standard parameters, and the predicted doublet rate based on our cell  
69 loading (5%). Doublets were removed and we then moved forward with only the predicted 'singlet'  
70 cells which constituted 95% of cells in each dataset. Each dataset was then re-normalized, scaled  
71 and dimensionally reduced using standard Seurat workflow. UMI, and mitochondrial content scores  
72 were regressed-out using Seurat's "ScaleData" function. The top 20 principal components from  
73 Seurat's "RunPCA" function were used to define the dimensions of the UMAP non-linear  
74 dimensional reduction analysis which was then viewed on a 2D UMAP plot. An unsupervised  
75 clustering analysis was also carried out using the same number of principal components. In order  
76 to identify the neuronal clusters in the dataset we used a set of established neuronal marker genes  
77 (*Tubb3*, *Snhg11*, *Nefl*, *Nefm*, *Nefh*) and genes known to be expressed early in SGN development  
78 (*Pou4f1*, *Gata3*, *Neurod1*). Although neuronal cells made up only a small proportion of the total  
79 cells (10-15%), cells within these clusters always overlapped with one another and were well  
80 separated from other clusters in the dataset. We additionally generated the top 10 markers for all  
81 clusters in the dataset and confirmed putative SGN clusters had a coherent neuronal expression  
82 pattern. SGN clusters were then isolated from each individual dataset.

83

84 Merging datasets: At each individual timepoint isolated SGN clusters were merged using Seurat's  
85 standard integration workflow to account for batch effects. For the integration of all timepoints  
86 together, SGN datasets for each timepoint were merged before carrying out the standard Seurat  
87 workflow for PCA analysis. Harmony (R Package v1.0)(6) integration was then applied to this  
88 dimensionally reduced Seurat object to account for batch effects between the individual datasets.  
89 For all merged objects, clustering analysis was re-done. Clusters were checked for quality and  
90 were removed if their identity could not be determined (< 3 significant genes defining their  
91 expression, low or no expression of neuronal marker genes, and/or top 10 marker genes matching  
92 > 1 cell type (eg: a mixture of glial and neuronal genes)). The 'nFeature\_RNA' (number of genes  
93 detected) and the batch origin of each cell was generated across each UMAP to ensure the dataset  
94 was not clustering based on either of these parameters after batch correction (Suppl fig 11).

95

96 Trajectory analysis: Slingshot (R package v1.8)(7) analysis was run using UMAP as the  
97 dimensionally reduced input. Slingshot uses a minimum spanning tree method to identify lineages  
98 of cells starting at the same origin and then diverging to unique endpoints. It then calculates  
99 pseudotime for all the cells on the lineage using principal curves. For all analyses, the start cluster  
100 was identified as the cluster containing the most immature SGNs defined by high expression of  
101 *Neurod1*. In the P1/E18 UMAP, E16 and whole combined datasets UMAP end clusters (Type 1A,  
102 B, C and Type 2) could be identified based on marker gene expression. For the E14 UMAP no end  
103 clusters were defined. In order to identify genes changing across pseudotime, tradeSeq (R package  
104 v1.4)(8) analysis was carried out on the E16/E18 Type 1A/2, E16 type B/C and E14 Slingshot  
105 trajectories with a Kknots value of 7 (E16/E18) or 8 (E14). For each dataset, tests were carried out  
106 to identify genes with gene expression patterns that were associated with pseudotime  
107 (associationTest), or had different expression patterns along the two lineages (patternTest), and  
108 genes that were differentially expressed at the endpoints of the lineages (diffEndTest). Additionally,  
109 in the E16/E18 Type 1A/2 dataset, we ran a test of genes differentially changing across the two

110 lineages as the Type 2 branch split from the Type 1A branch (earlyDETest between knots 3 and  
111 7).

112

113 Monocle 3 analysis: Monocle 3 (R package) (9, 10) analysis was undertaken on the E14 dataset in  
114 order to test whether the same E14 dataset clusters were identified when using an alternative  
115 approach to Seurat. Raw gene counts for the E14 SGN dataset were extracted from the Seurat  
116 object. The standard Monocle 3 workflow was then applied to this raw data including  
117 preprocessing, removal of batch effects using mutual nearest neighbor alignment (11) and  
118 dimensional reduction and UMAP visualization of the data. A clustering analysis was undertaken  
119 and the top 10 marker genes for each cluster were calculated.

120

121 SCENIC regulon analysis: SCENIC (12) analysis was carried out as described in Kolla et al.  
122 (2020)(13). Briefly, SCENIC was run on datasets in which every 5-20 cells had been randomly  
123 pooled and gene expression averaged. Activity of a regulon within a specific cluster was assessed  
124 by both their regulon specificity score (RSS) and their AUCcell scores, with only regulons significant  
125 in both tests considered active.

126

127 Immunohistochemistry and smFISH: Cochleae were collected at E14, E16, E18 and P1 and fixed  
128 in 4% PFA for 2 hours (immunohistochemistry) or overnight (smFISH). For sections, tissue was  
129 collected from either CD1 or MAPT<sup>EGFP</sup> animals (where quantification was required), and  
130 cryoprotected through a gradient of sucrose (5%, 10%, 15%, 20%, 25% and 30%). Samples were  
131 embedded in Tissue-Tek O.C.T compound and sectioned at 12 µm. For whole mounts, cochleae  
132 were dissected to expose the sensory epithelium and SG.

133

134 Immunohistochemistry: Sections and whole mounts were blocked for 1 hour in 10% normal donkey  
135 serum diluted in 0.5% triton-X in PBS. If the primary antibody was raised in mouse, then the  
136 blocking solution would also include 0.5% Unconjugated AffiniPure FAB fragment goat Anti-mouse

137 IgG (H L) (Jackson ImmunoResearchLabs). Primary antibody was added at the appreciate  
138 concentration (Suppl. Table 1) and incubated overnight. Tissue was then washed 3 times in PBS  
139 followed by incubation with AlexaFluor-conjugated secondary antibodies (1:500) diluted in blocking  
140 solution for 2 hours. Tissue was washed and cover slipped/mounted using Fluoromount-G. Antigen  
141 retrieval was carried out on POU4F1 and ESPN antibodies prior to initial blocking step by incubating  
142 slides in near boiling citrate buffer (10mM citric acid, 0.05% Tween20, pH6) for 5 minutes.

143

144 smFISH: For smFISH, gene specific probes were ordered from Advanced Cell Diagnostics (Suppl.  
145 Table 2) and the RNAscope® Fluorescent Multiplex Reagent Kit (320851) was run following  
146 manufacturer's instructions on sections. For slides where smFISH was being quantified an  
147 additional immunohistochemistry step labelling for GFP was added to the end of the protocol, using  
148 the standard immunohistochemistry protocol described above. For whole mounts RNAscope was  
149 run using a previously published protocol(14) followed by immunohistochemistry staining for  
150 ZSGreen using the standard protocol described above.

151

152 Cell count data analysis: For all cell counts, sections were imaged with identical confocal  
153 microscopy settings across all slides. Negative control slides were used to threshold out  
154 background in both immunohistochemistry and RNAScope experiments. Images were imported  
155 into ImageJ (15) software and using only the neuronal marker and DAPI signal cells were hand  
156 counted as a neuron if they colocalized both the marker and DAPI. Each identified neuron was then  
157 counted for presence or absence of additional markers via presence of signal above background  
158 levels. For RNAScope this was determined as >3 punta per cell using the negative control probe  
159 provided in the kit.

160

161 TH cell counts:

162 Whole mount: Whole mount TH immunohistochemistry was combined with genetic sparse labelling  
163 using *Neurog1*<sup>CreERT2</sup>*R26R*<sup>mT/mG</sup> to quantify the proportion of TH expressing SGNs that were Type

164 1 or Type 2. TH<sup>+</sup> neurons were identified using TH immunostaining of their cell bodies. The  
165 peripheral process of each TH<sup>+</sup> neuron was then traced to its terminus either at the level of the  
166 inner hair cells (Type 1) or outer hair cells (Type 2) based on GFP labeling. Counts represent 20  
167 TH<sup>+</sup> neurons counted from pups across 4 litters.

168 Sections: The proportion of SGNs expressing TH across development was assessed by counting  
169 the total number of TH<sup>+</sup> and TH<sup>-</sup> SGNs in a modiolar section through the cochlea at each time  
170 point using Neurofilament (NF) and TH immunolabelling. Counts were combined totals across all  
171 three turns of the SG for 5 pups from separate litters. Data presented as mean  $\pm$  SEM. Statistical  
172 test is one-way ANOVA followed by Tukey's multiple comparison's test.

173

174 E18 SGN subgroup marker quantification: The proportion of SGNs expressing either Calb2/Lypd1  
175 RNA, *Tle4/Lypd1* RNA or CALB1/CALB2 protein at E18 were assessed by counting the number of  
176 positive SGNs for each marker against the total number of SGNs labelled with either GFP (using  
177 MAPT<sup>EGFP</sup> tissue) or TUJ1 (using wildtype CD1 tissue). The proportion of POU4F1<sup>+</sup> SGNs  
178 expressing ESPN was counted similarly, with the total number of POU4F1<sup>+</sup>/ESPN<sup>+</sup> SGNs against  
179 the total number of POU4F1<sup>+</sup> SGNS. Counts were taken from the basal turn in a mid-modiolar  
180 section from the middle of the confocal image stack. Counts were combined totals for 3 pups from  
181 separate litters. Data presented as mean  $\pm$  SEM.

182

183 Data availability: Single-cell gene expression data have been deposited in the Gene Expression  
184 Omnibus data repository under accession code: GSE195500. Gene by cell expression matrix and  
185 data visualizations presented in this paper will be available through the gEAR Portal.

186

187

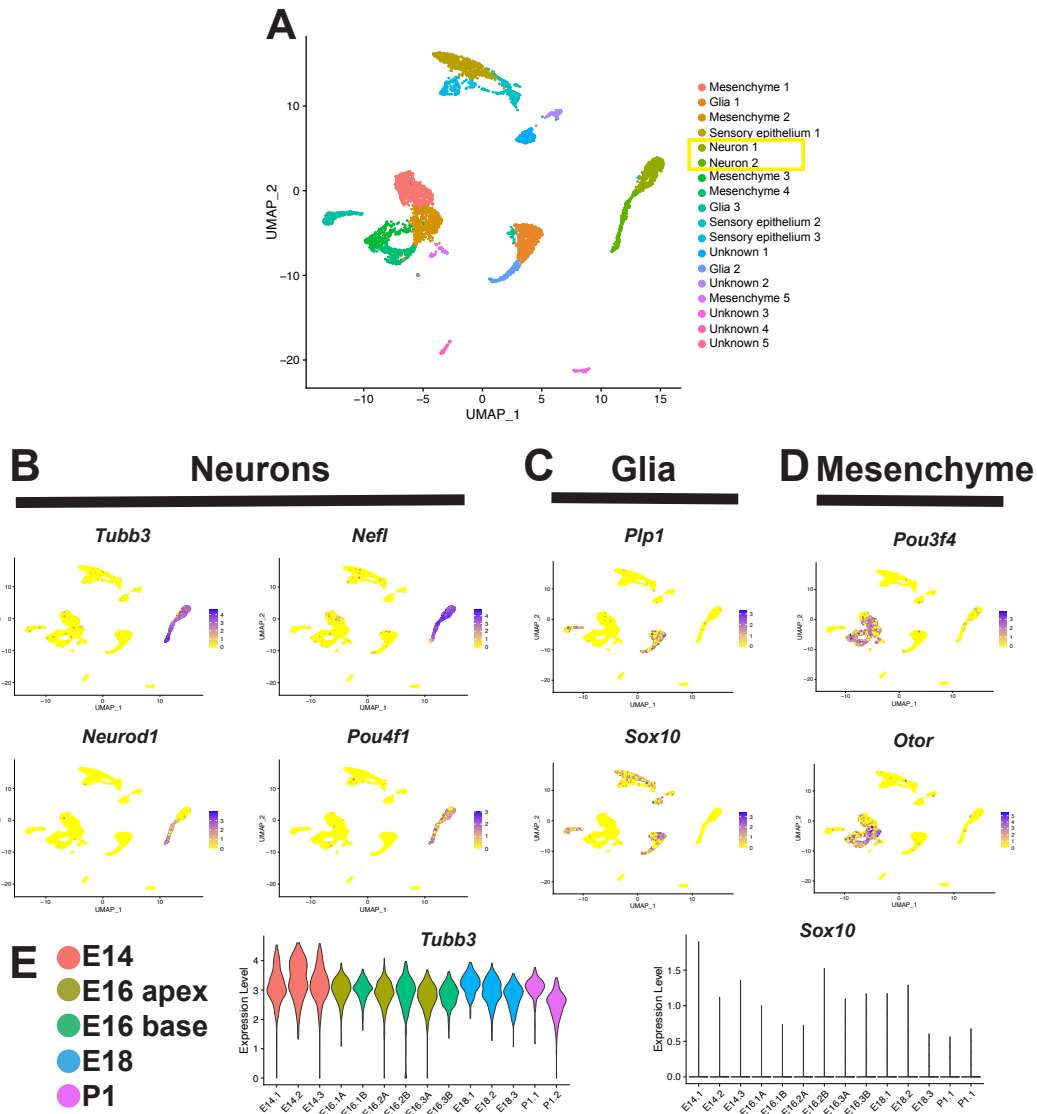
188

- 189 1. E. J. Koundakjian, J. L. Appler, L. V. Goodrich, Auditory neurons make stereotyped wiring  
190 decisions before maturation of their targets. *Journal of Neuroscience* **27**, 14078-14088  
191 (2007).
- 192 2. J. A. Harris *et al.*, Anatomical characterization of Cre driver mice for neural circuit  
193 mapping and manipulation. *Frontiers in Neural Circuits* **8** (2014).
- 194 3. K. L. Tucker, M. Meyer, Y.-A. Barde, Neurotrophins are required for nerve growth during  
195 development. *Nature neuroscience* **4**, 29-37 (2001).
- 196 4. T. Stuart *et al.*, Comprehensive integration of single-cell data. *Cell* **177**, 1888-1902.  
197 e1821 (2019).
- 198 5. C. S. McGinnis, L. M. Murrow, Z. J. Gartner, DoubletFinder: doublet detection in single-  
199 cell RNA sequencing data using artificial nearest neighbors. *Cell systems* **8**, 329-337.  
200 e324 (2019).
- 201 6. I. Korsunsky *et al.*, Fast, sensitive and accurate integration of single-cell data with  
202 Harmony. *Nature methods* **16**, 1289-1296 (2019).
- 203 7. K. Street *et al.*, Slingshot: cell lineage and pseudotime inference for single-cell  
204 transcriptomics. *BMC genomics* **19**, 1-16 (2018).
- 205 8. K. Van den Berge *et al.*, Trajectory-based differential expression analysis for single-cell  
206 sequencing data. *Nature communications* **11**, 1-13 (2020).
- 207 9. J. Cao *et al.*, The single-cell transcriptional landscape of mammalian organogenesis.  
208 *Nature* **566**, 496-502 (2019).
- 209 10. X. Qiu *et al.*, Reversed graph embedding resolves complex single-cell trajectories. *Nature*  
210 *methods* **14**, 979-982 (2017).
- 211 11. L. Haghverdi, A. T. Lun, M. D. Morgan, J. C. Marioni, Batch effects in single-cell RNA-  
212 sequencing data are corrected by matching mutual nearest neighbors. *Nature*  
213 *biotechnology* **36**, 421-427 (2018).
- 214 12. S. Aibar *et al.*, SCENIC: single-cell regulatory network inference and clustering. *Nature*  
215 *methods* **14**, 1083-1086 (2017).
- 216 13. L. Kolla *et al.*, Characterization of the development of the mouse cochlear epithelium at  
217 the single cell level. *Nature communications* **11**, 1-16 (2020).
- 218 14. J. Kersigo *et al.*, A RNAscope whole mount approach that can be combined with  
219 immunofluorescence to quantify differential distribution of mRNA. *Cell and tissue*  
220 *research* **374**, 251-262 (2018).
- 221 15. J. Schindelin *et al.*, Fiji: an open-source platform for biological-image analysis. *Nature*  
222 *methods* **9**, 676-682 (2012).

223

224





225

226

**Fig. S1.**

227 **Identification of developing SGNs.** **A.** UMAP displaying results from a single cell  
 228 collection at E14 that includes 5,225 cells after initial QC and doublet removal. Legend  
 229 indicates identities of clusters containing SGNs (yellow box), glia, mesenchyme, and  
 230 sensory epithelium. Remaining cell clusters have not been identified. **B.** Feature plots of  
 231 the same projection as in **A** displaying the expression of specific markers for SGNs (**B**),  
 232 glia (**C**), and mesenchyme (**D**). **E.** Violin plots displaying the expression of the neuronal  
 233 marker *Tubb3*, and the glial marker *Sox10* across the identified SGN clusters from each  
 234 collection. The high expression of *Tubb3* and negligible expression of *Sox10* indicates the  
 235 SGN clusters are free of glial contamination.

236

237  
238  
239  
240  
241  
242  
243  
244  
245  
246  
247  
248  
249  
250

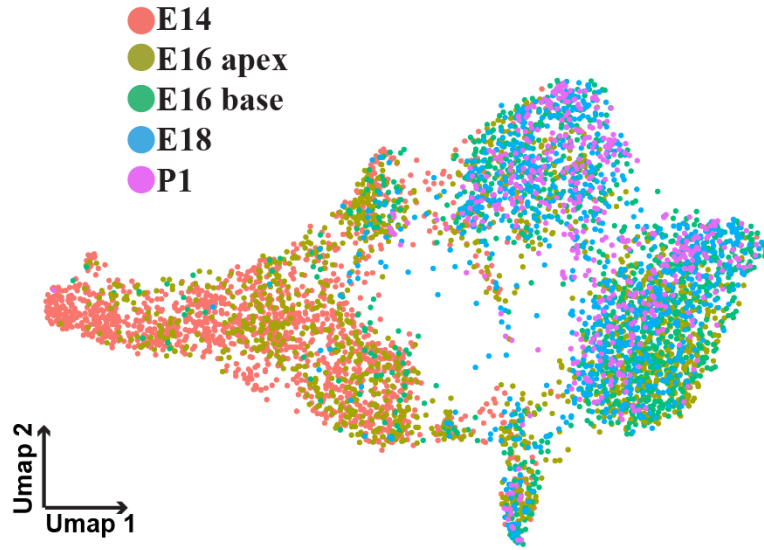
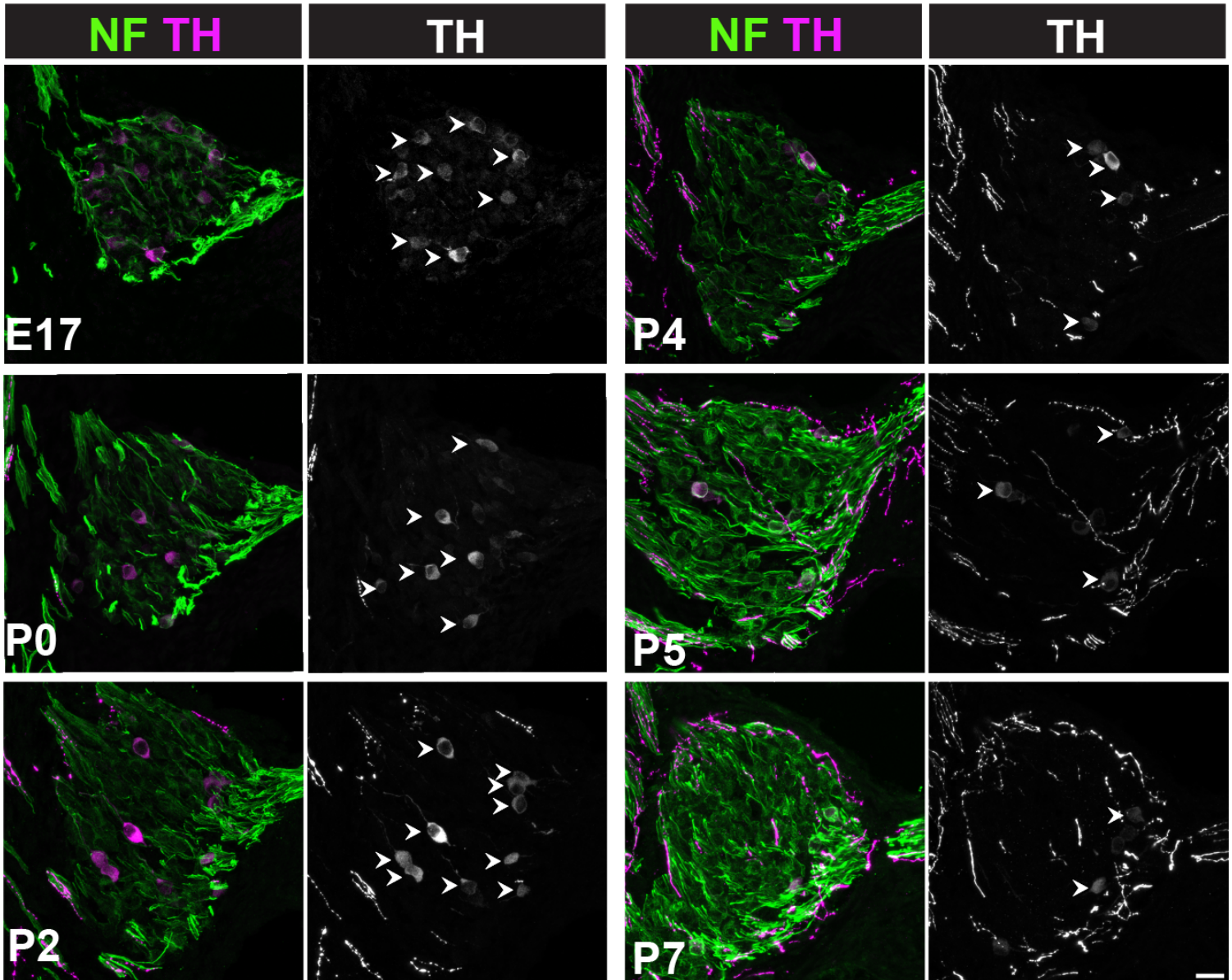


**Fig. S2.**

**Combined SGN dataset.** UMAP plot of 5,441 SGNs collected at E14, E16, E18 and P1 colored by the timepoint. Note that cells from each timepoint form a gradient from most immature to most mature along the UMAP 1 axis.



251

252 **Fig. S3.**

253 **Timecourse of TH expression in the perinatal SG.** Images of TH and Neurofilament  
 254 immunolabeling in the mid SG from E17-P7. The number of TH positive SGNs drops  
 255 after P4. Arrowheads point to TH positive cell bodies. Scale bar, 20 $\mu$ m.  
 256

257

258  
259  
260  
261  
262  
263  
264  
265  
266  
267  
268  
269  
270  
271  
272  
273  
274  
275  
276  
277  
278  
279  
280  
281  
282

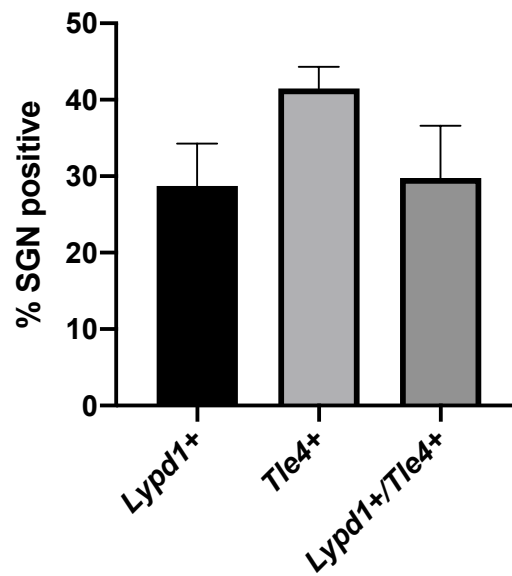
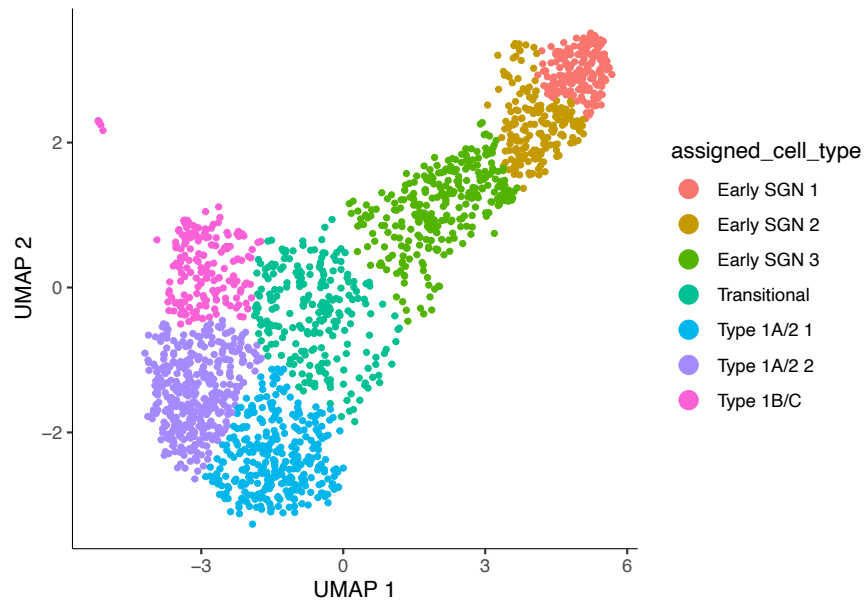


**Fig. S4.**

**Proportion of Tle4+ and Lypd1+ SGNs at E18.** Quantification of proportion of SGNs expressing each marker at E18. About 30% of SGNs express both Lypd1 and Tle4 to some degree while the remaining 70% express either Lypd1 only or Tle4 only. Data presented as mean  $\pm$  SEM.

283

284



295

**Fig. S5.**

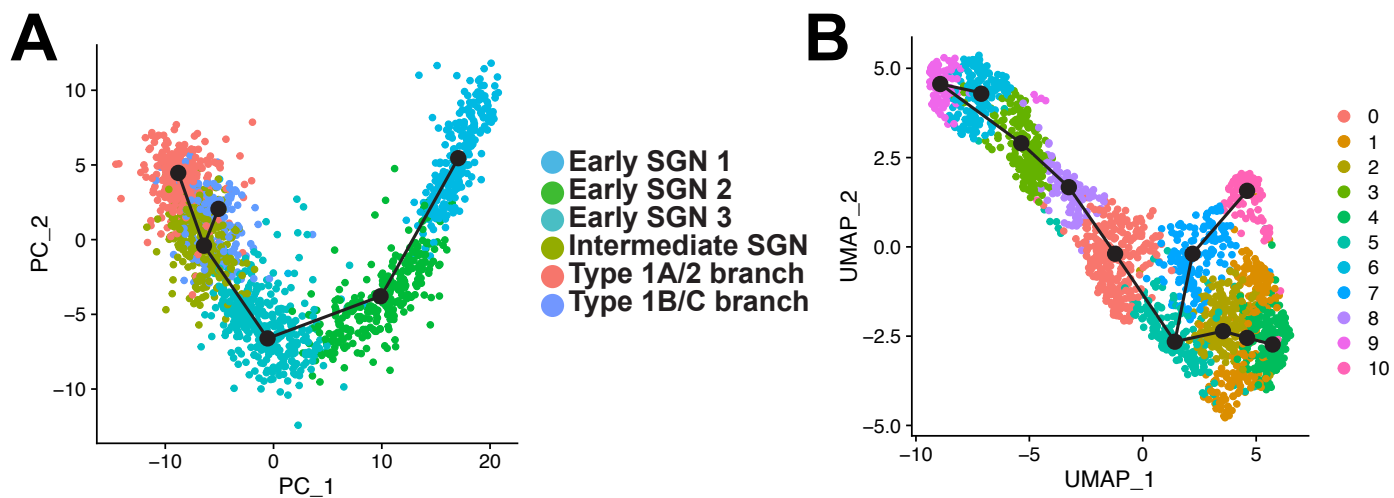
296

**Monocle analysis at E14.** Analysis of E14 dataset using Monocle reveals equivalent

297

early SGN clusters.

298



299

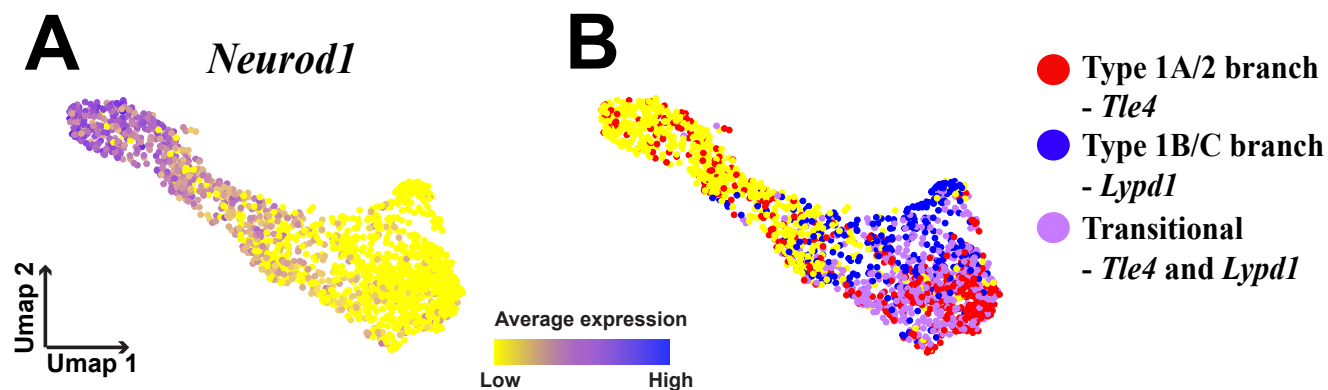
300 **Fig. S6**

301 **Slingshot analysis at E14.** Modulation of Slingshot by (A) using PCA as an input, or (B)  
 302 over clustering the dataset, does not alter the finding of an E14 split between Type 1A/2  
 303 and Type 1B/C precursors.

304

305

306



307

308 **Fig. S7.**

309 **Gene expression defines clusters at E14.** **a.** Feature plot of the E14 dataset showing  
310 *Neurod1* expression is highest in the Early SGN 1 cluster. **b.** Feature plot of the E14  
311 dataset displaying binarized expression of *Tle4* and *Lypd1* in two spatially separated  
312 clusters in the more mature neurons in the dataset. Some neurons in a transitional phase  
313 are expressing both markers.

314

315

316

317

318

319

320

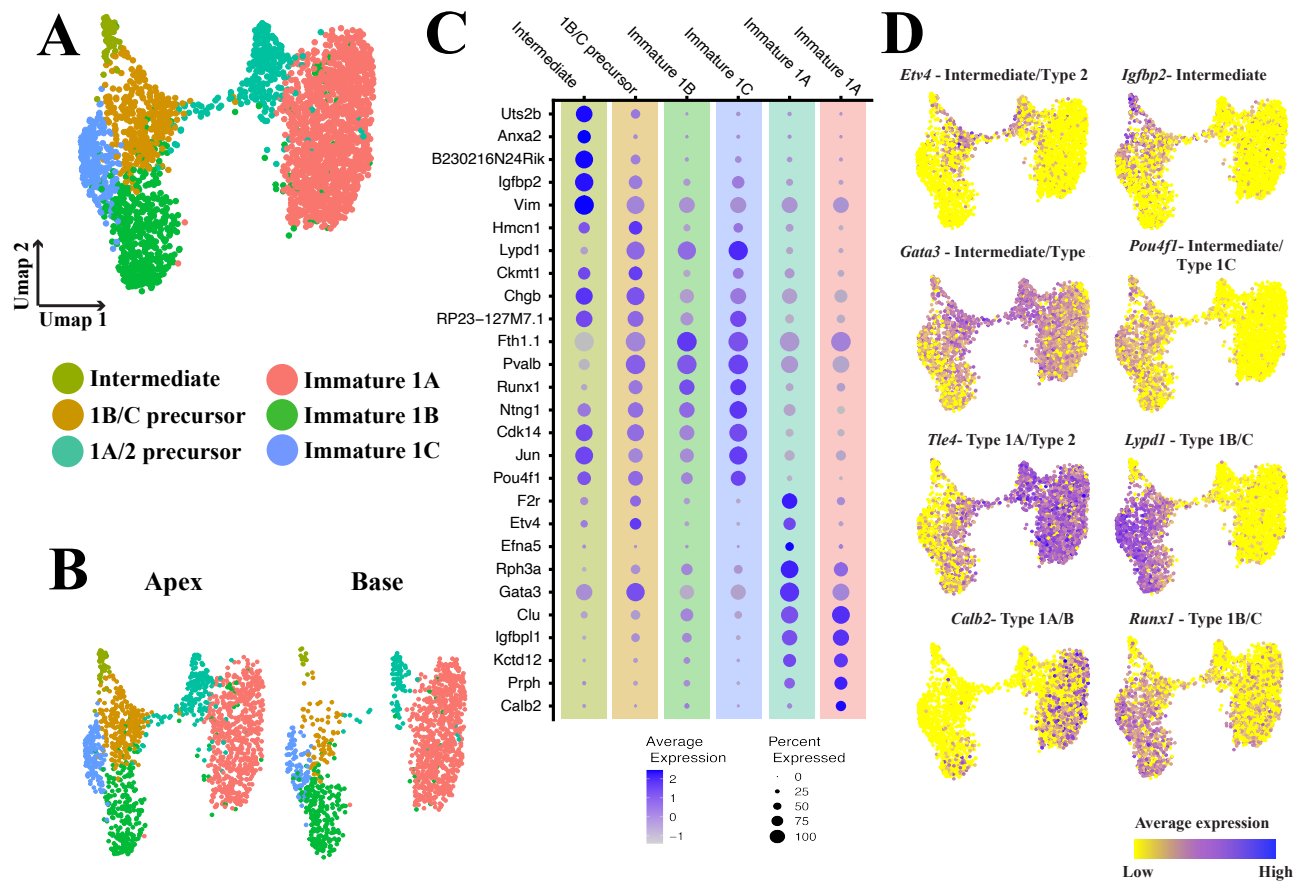
321

322

323

324

325

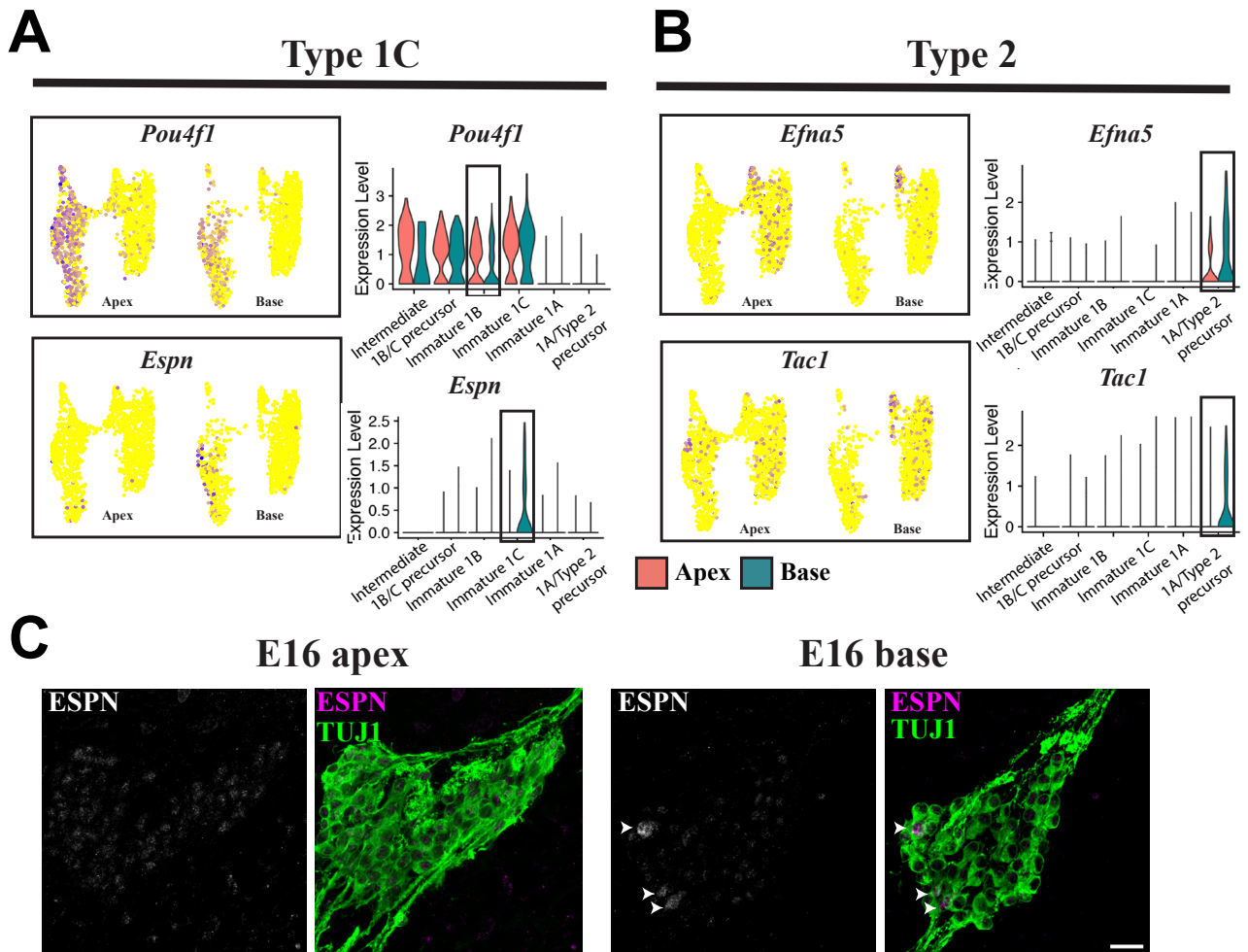


326  
327  
328  
329  
330  
331  
332  
333  
334

**Fig. S8.**

**Characterization of the E16 dataset.** **A.** UMAP of 2,702 SGNs collected from the base and apical portions of the SG with cluster identities indicated. **B.** UMAP in (A) split by SGNs originating in the apex and base. **C.** Dot plot showing the top 5 differentially expressed markers for each of the clusters identified in (A). **D.** Feature plots of gene markers for the clusters identified in (A).





335

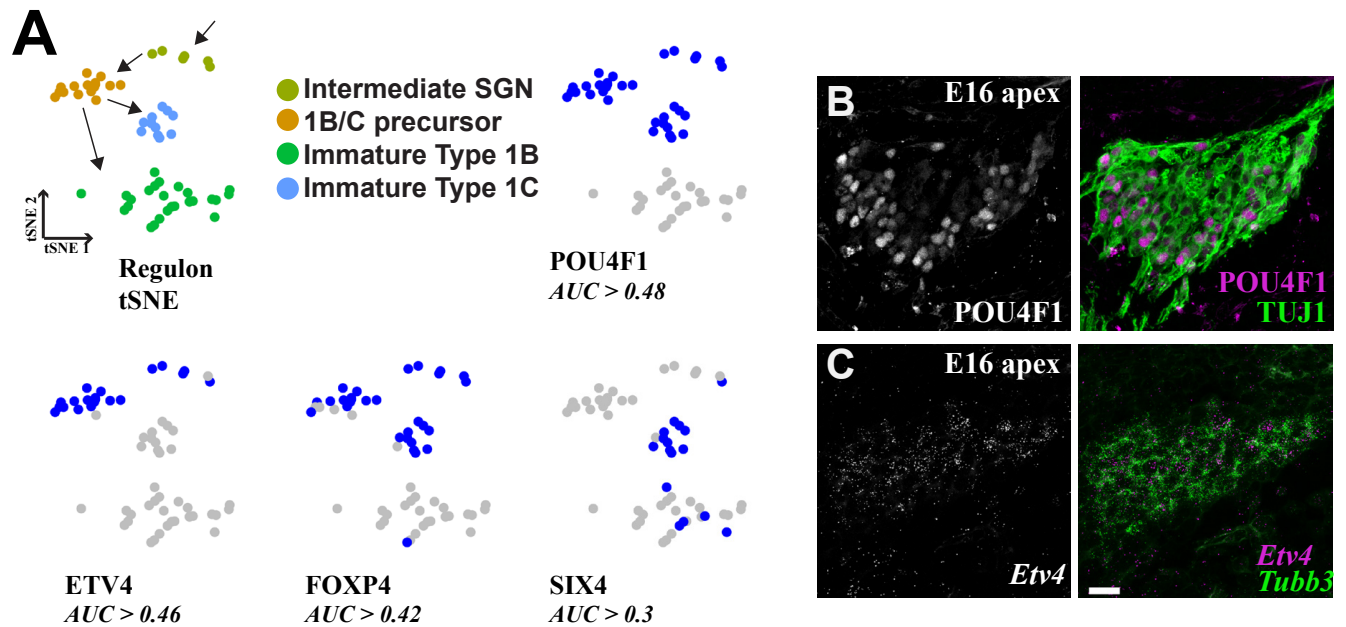
336 **Fig. S9.**

337 **Type 1C and Type 2 SGNs are identifiable at E16.** A-B. Feature plots (left) and violin  
 338 plots (right) of E16 dataset from **Suppl. Fig 7** split by apex and base, displaying Type 1C  
 339 (A) and Type 2 (B) marker gene expression. Boxes on violin plots indicate *Pou4f1*  
 340 expression decreasing in the 1B cluster in the more mature basal neurons, and the other 3  
 341 genes all turning on in the basal neurons in either the Type 1C or Type 2 clusters. C  
 342 immunohistochemistry confirms Type 1 C marker ESPN turns on expression in basal  
 343 SGNs. Scale bar in all images indicates 20 $\mu$ m.

344

345

346



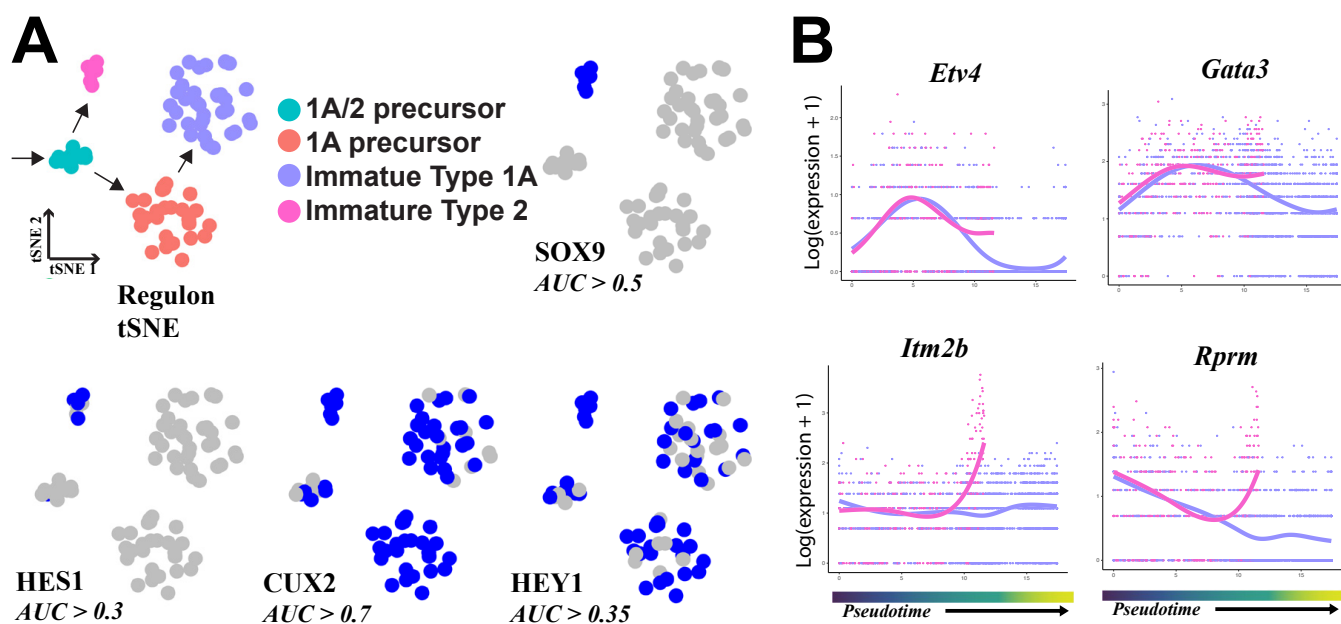
347

348 **Fig. S10.**

349 **Regulon analysis in E16 1B/C dataset.** A Top row: tSNE plot based on identification of  
 350 transcriptional regulons using SCENIC. Clusters are colored based on their identification  
 351 in **fig 7A**. Arrows indicate order of specification based on Slingshot analysis. Regulon  
 352 tSNE plot of POU4F1 shows activity in early and 1C SGN clusters, blue dots indicate the  
 353 regulon is active. Bottom Row: examples of other regulons which were both significantly  
 354 restricted to specific clusters, and were predicted to be active based AUC thresholding  
 355 (see methods). **B.** immunohistochemistry confirms POU4F1 expression in a subset of  
 356 SGNs at E16. **C.** smFISH confirms *Etv4* expression in the SG at E16. Scale bar in **C.**  
 357 (same as **B.**) indicates 20 $\mu$ m.

358

359



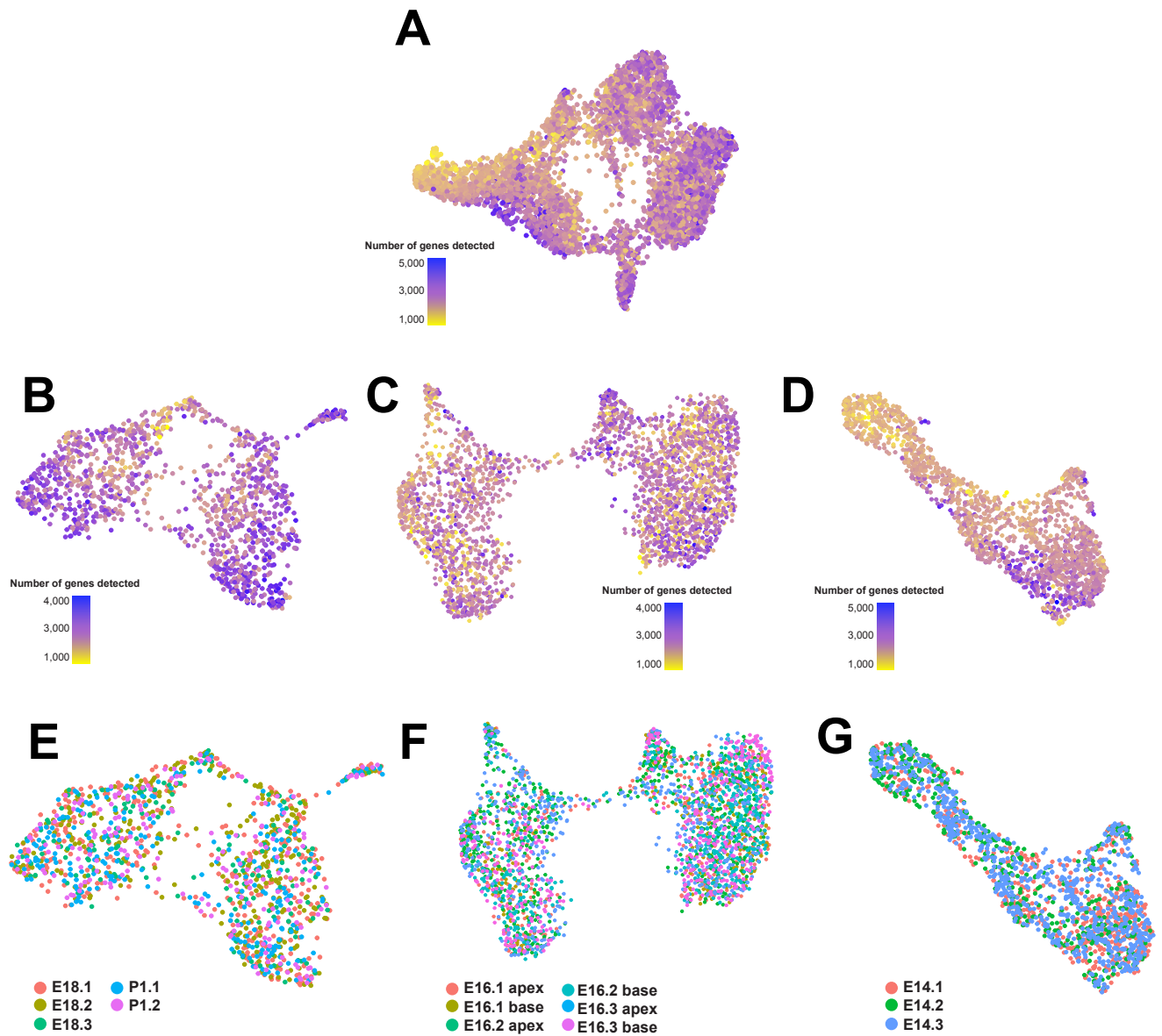
360

361 **Fig. S11.**

362 **Regulon and tradeSeq analysis in E16/18 1A/2 dataset.** **a** Top row: tSNE plot based on  
 363 identification of transcriptional regulons using SCENIC. Clusters are colored based on  
 364 their identification in **fig 7D**. Arrows indicate order of specification based on Slingshot  
 365 analysis. Regulon tSNE plot of SOX9 shows specific activity in Type 2 cluster, blue dots  
 366 indicate the regulon is active. Bottom Row: examples of other regulons which were both  
 367 significantly restricted to specific clusters, and were predicted to be active based AUC  
 368 thresholding (see methods). **B**. Plots of the expression of genes identified by tradeSeq  
 369 analysis as differentially expressed along the two trajectories (top row) and as the two  
 370 lineages split (bottom row).

371

372



373  
374

375  
376

377 **Fig. S12.**  
378 **Dataset do not cluster based on gene detection rate and batch.** UMAPs displaying the  
379 number of genes detected per cell and the batch identity of each cell in the whole  
380 combined dataset (A), E18/P1 combined dataset (B,E), E16 dataset (C,F), and E14  
381 dataset (D,G).

382  
383

384  
385

386 **Table S1.**

387 **List of antibodies used for immunohistochemistry**

<b>Antibody</b>	<b>Concentration</b>	<b>Source</b>	<b>Cat#</b>
Rabbit anti-CALB1	1:200	Millipore	AB1778
Rabbit anti-TUJ1	1:1000	Sigma-Aldrich	T2200
Mouse anti-CALB2	1:500	Millipore/Chemicon	MAB1568
Rabbit anti-ESPN	1:200	Invitrogen	PA5-55941
Mouse anti-POU4F1	1:100	Millipore	MAB1585
Rabbit anti-ZSGreen	1:500	Takara Bio, USA	632474
Chicken anti-GFP	1:500	GeneTex	GTX26662
Rabbit anti-TH	1:500	Millipore	AB152
Chicken anti-Neurofilament L,M,H	1:1000	Aves Labs	NFL, NFM, NFH

388

389

**Table S2.**

390

**List of probes used for single molecule fluorescent *in situ* hybridization**

391

<b>Probe</b>	<b>Source</b>	<b>Catalog #</b>
Mm-Calb2	ACDBio	313641
Mm-Lypd1	ACDBio	318361
Mm-Efna5	ACDBio	316641
Mm-Tle4	ACDBio	417301
Mm-Etv4	ACDBio	458121
Mm-Tubb3	ACDBio	423391

392 **Dataset S1. (separate file)**

393 **Description:** Top 50 differentially expressed genes in each cluster for each dataset (combined,  
394 E14, E16, E18/P1, E18/P1 Type 1 vs Type 2).

395

396 **Dataset S2. (separate file)**

397 **Description:** Top 100 differentially expressed genes from tradeSeq analysis for the E14 dataset.

398

399 **Dataset S3. (separate file)**

400 **Description:** Top 100 differentially expressed genes from tradeSeq analysis for the E16 Type  
401 1B/C lineage dataset.

402

403 **Dataset S4. (separate file)**

404 **Description:** Top 100 differentially expressed genes from tradeSeq analysis for the E16/E18 Type  
405 1A/2 lineage dataset.

406

407 **Dataset S5. (separate file)**

408 **Description:** List of SCENIC regulons expressed for each cluster in the E14 dataset.

409

410 **Dataset S6. (separate file)**

411 **Description:** List of SCENIC regulons expressed for each cluster in the E16 dataset.

412

413 **Dataset S7. (separate file)**

414 **Description:** List of SCENIC regulons expressed for each cluster in the E16/E18 dataset

415

416 **Dataset S8. (separate file)**

417 **Description:** Initial 'mean reads per cell', 'median genes per cell' and 'number of reads'  
418 sequencing data from the Cell Ranger output

419